3-2023

Synthesis, Structural, Magnetic and Computational Studies of a One-Dimensional Ferromagnetic Cu(II) Chain Assembled from a New Schiff Base Ligand

Anne Worrell

Gabriele Delle Monache

Mark M. Turnbull

Jeremy M. Rawson

Theocharis C. Stamatatos

See next page for additional authors

Authors

Anne Worrell, Gabriele Delle Monache, Mark M. Turnbull, Jeremy M. Rawson, Theocharis C. Stamatatos, and Melanie Pilkington

chemistry

MDPI

Article

Synthesis, Structural, Magnetic and Computational Studies of a One-Dimensional Ferromagnetic Cu(II) Chain Assembled from a New Schiff Base Ligand

Anne Worrell [1], Gabriele Delle Monache [1], Mark M. Turnbull [2], Jeremy M. Rawson [3], Theocharis C. Stamatatos [4,*] and Melanie Pilkington [1,*]

[1] Department of Chemistry, Brock University, 1812 Sir Isaac Brock Way, St. Catharines, ON L2S 3A1, Canada
[2] Carlson School of Chemistry and Biochemistry, Clark University, 950 Main St., Worcester, MA 01610, USA
[3] Department of Chemistry and Biochemistry, University of Windsor, 401 Sunset Ave, Windsor, ON N9B 3P4, Canada
[4] Department of Chemistry, University of Patras, 26504 Patras, Greece
* Correspondence: thstama@upatras.gr (T.C.S.); mpilkington@brocku.ca (M.P.)

Abstract: A new asymmetrically substituted ONOO Schiff base ligand N-(2′-hydroxy-1′-naphthylidene)-3-amino-2-naphthoic acid (**nanc**H_2) was prepared from the condensation of 2–hydroxy–1–naphthaldehyde and 3–amino–2–naphthoic acid. **nanc**H_2 reacts with $Cu_2(O_2CMe)_4{\cdot}2H_2O$ in the presence of $Gd(O_2CMe)_3{\cdot}6H_2O$ to afford a uniform one-dimensional homometallic chain, $[Cu^{II}(\mathbf{nanc})]_n$ (**1**). The structure of **1** was elucidated via single crystal X-ray diffraction studies, which revealed that the Cu(II) ions adopt distorted square planar geometries and are coordinated in a tridentate manner by an [ONO] donor set from one **nanc**$^{2-}$ ligand and an O^- of a bridging carboxylate group from a second ligand. The bridging carboxylato group of the **nanc**$^{2-}$ ligand adopts a syn, anti-η^1:η^1:μ conformation linking neighboring Cu(II) ions, forming a 1D chain. The magnetic susceptibility of **1** follows Curie–Weiss law in the range 45–300 K (C = 0.474(1) emu K mol-1, θ = +7.9(3) K), consistent with ferromagnetic interactions between $S = \frac{1}{2}$ Cu(II) ions with g = 2.248. Subsequently, the data fit well to the 1D quantum Heisenberg ferromagnetic (QHFM) chain model with g = 2.271, and J = +12.3 K. DFT calculations, implementing the broken symmetry approach, were also carried out on a model dimeric unit extracted from the polymeric chain structure. The calculated exchange coupling via the carboxylate bridge (J = +13.8 K) is consistent with the observed ferromagnetic exchange between neighbouring Cu(II) centres.

Keywords: Cu(II); Schiff base; aromatic ligands; ferromagnetic interactions; one-dimensional uniform chain; coordination polymer; DFT studies

Citation: Worrell, A.; Delle Monache, G.; Turnbull, M.M.; Rawson, J.M.; Stamatatos, T.C.; Pilkington, M. Synthesis, Structural, Magnetic and Computational Studies of a One-Dimensional Ferromagnetic Cu(II) Chain Assembled from a New Schiff Base Ligand. *Chemistry* **2023**, *5*, 85–96. https://doi.org/10.3390/chemistry5010007

Academic Editor: Konstantis Konidaris

Received: 30 November 2022
Revised: 3 January 2023
Accepted: 5 January 2023
Published: 7 January 2023

1. Introduction

Coordination polymers have garnered significant interest due to their potential for displaying fascinating magnetic behaviour [1–8], and have found applications in various fields, including catalysis [9] and medicinal chemistry [10], among others [11–13]. There has been considerable attention paid towards low-dimensional materials which can exhibit unusual forms of magnetic response, depending on the dimensionality of the exchange pathway and the type of spin system. These can lead to examples of spin frustration [14,15], Koesterlitz–Thouless transitions in two-dimensional systems [16,17], and the emergence of Haldane gaps in one-dimensional chains [18,19]. One-dimensional materials comprise examples of both regular chains (a single exchange term), or alternating chains (comprising two magnetic exchange terms which may be ferromagnetic, antiferromagnetic, or a mixture of both ferro- and antiferromagnetic) [20,21]. When Ising-like spins are involved, such systems can lead to 'single chain magnets' in which there is a gapped state with slow

relaxation [22,23]. Some of the most well-studied low-dimensional models comprise one-dimensional (1D) Heisenberg $S = \frac{1}{2}$ magnetic compounds [24–26]. In this respect, the magnetic insulator copper pyrazine dinitrate has provided a unique opportunity for a quantitative comparison between theory and experiment [26]. For such isotropic spins, a unique expression for their susceptibility is not possible, but expressions in the case of both antiferromagnetic and ferromagnetic exchange have been put forward. In the case of ferromagnetic exchange, such regular 1D chains can be well-described by the 1D quantum Heisenberg ferromagnet (1D QHFM) equation (Equation (1)), defined by the Hamiltonian in Equation (2) [27–29]. The values of the numerator (N_i) and denominator (D_i) in Equation (1) are tabulated elsewhere [30]. Cu(II)-based polymers provide good models for exploring such behaviour [31–33], and comprise one of the most well-studied 1D systems to date [26,34–37].

$$\chi_{mol}(1 - D\ QHFM) = \frac{C_{mol}}{T}\left[\frac{1 + \sum_{i=1}^{3} N_i \left(\frac{J}{k_B T}\right)^i}{1 + \sum_{i=1}^{4} D_i \left(\frac{J}{k_B T}\right)^i}\right] \quad (1)$$

$$H = -JS_i \cdot S_j \quad (2)$$

Molecular self-assembly of 3*d* metal ion complexes with polydentate ligands has been shown to be an effective method of generating coordination polymers [38–42]. Schiff bases are particularly appealing as they have been reported to exhibit valuable properties, lending themselves to the formation of compounds with a broad range of industrial and biological applications [43–50]. Thus, this class of ligands are attractive and can be readily synthesized from the condensation reaction between an amine and a carbonyl compound. The incorporation of one or more donor atoms into the Schiff base backbone affords polydentate ligands which can stabilize complexes with various transition metals due to the chelate effect [51–57]. Moreover, including hydroxy or carboxylate functional groups provides bridging ligands to construct coordination clusters or polymers and has proven to be an effective approach [58–61], exemplified by Schiff bases with a naphthalene-based organic scaffold which have been successfully used to isolate 1-D magnetic chains [62–65]. In the current study, we utilized the new tetradentate chelating/bridging Schiff base ligand N-(2′-hydroxy-1′-naphthylidene)-3-amino-2-naphthoic acid (**nanc**H_2), (Scheme 1) in Cu(II) coordination chemistry, through utilizing the serendipitous assembly approach. As mentioned previously, these systems provide excellent models for studying fundamental magnetic behaviour in 1D systems that are strongly correlated to the magnetic exchange pathway and the type of spin system. To expand our fundamental understanding of such systems, we report herein the synthesis, magnetostructural, and DFT studies of a new, one-dimensional chain, $[Cu^{II}(\mathbf{nanc})]_n$ (**1**).

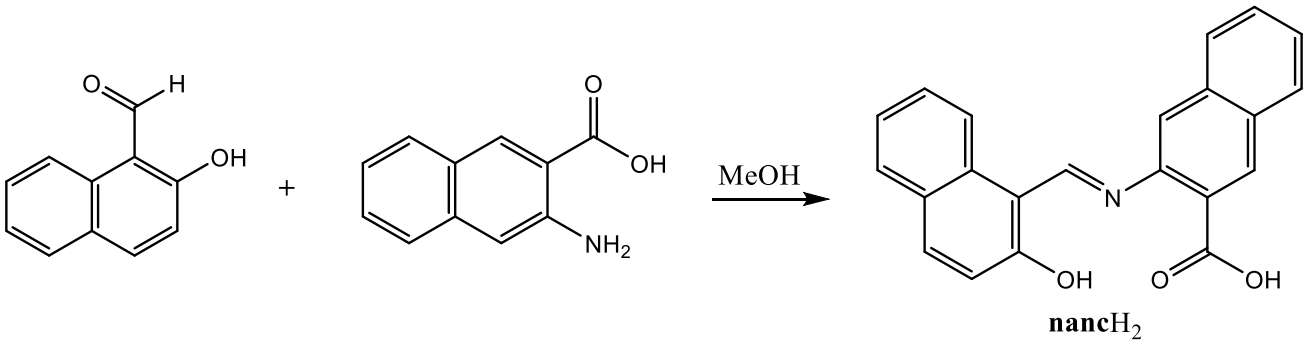

Scheme 1. Synthesis of the Schiff base ligand, **nanc**H_2.

2. Materials & Methods

General Considerations: All manipulations were performed under aerobic conditions using materials (reagent grade) and solvents as received from Sigma-Aldrich. Elemental analyses were carried out on a PerkinElmer 2400 Combustion CHN Analyser. IR spectra were obtained on solid samples using a Bruker Alpha FT-IR spectrometer, equipped with ALPHA's Platinum ATR single reflection module. Electrospray ionization (ESI) mass spectra were acquired from a DCM/MeOH solution of nancH_2 by utilizing a Bruker Avance DPX-400 MHz instrument. The NMR spectra were obtained using a Bruker AVANCE III HD 400 MHz in DMSO-d_6 solvent. The NMR spectra are reported relative to tetramethylsilane (δ = 0 ppm).

Preparation of N-(2′-hydroxy-1′-naphthylidene)-3-amino-2-naphthoic acid (nancH_2): 2–Hydroxy–1–naphthaldehyde (2.58 g, 15 mmol) and 3–amino–2–naphthoic acid (2.78 g, 15 mmol) were added to methanol (40 mL) and refluxed for 2 h. A yellow powder was isolated by filtration and dried in air. Yield (3.58 g, 70%). Mp 268 °C; ^{1}H NMR (ppm, DMSO-d_6) 6.86 (d, 1H), 7.32 (t, 1H), 7.51–7.74 (m, 4H), 7.87 (d, 1H), 8.07 (dd, 2H), 8.44 (t, 2H), 8.62 (s, 1H), 9.51 (s, 1H). ^{13}C NMR (ppm, DMSO-d_6) 108.9 (CH-$C_9H_6CO_2H$), 116.4 (CH-C_9H_7O), 120.2 (CH-$C_9H_6CO_2H$), 122.1 (CH-C_9H_7O), 123.5 (CH-$C_9H_6CO_2H$), 123.9 (CH-$C_9H_6CO_2H$), 126.3 (C-C=N), 126.4 (CH-C_9H_7O), 127.4 (C-C_9H_8O), 128.2 (C-$C_9H_7CO_2H$), 128.8 (C-$C_9H_7CO_2H$), 129.9 (C-C_9H_8O), 132.4 (CH-C_9H_7O), 133.7 (CH-C_9H_7O), 135.2 (C-OH), 138.0 (C-CO_2H), 139.7 (C-N), 167.4 (C=N), 174.7 (C=O). Mass spectrum (*m/z*, ESI$^-$): 339.9(M-1). IR data (cm^{-1}): 2995, 1702, 1628, 1604, 1588, 1544, 1491, 1459, 1408, 1370, 1346, 1302, 1246, 1214, 1195, 1142, 1043, 974, 925, 866, 840, 786, 747, 732, 689, 655, 628, 584, 566, 555, 525, 503, 470, 423, 408.

Preparation of [Cu^{II}(nanc)]$_n$ (1): $Cu_2(O_2CMe)_4{\cdot}2H_2O$ (0.04 g, 0.1 mmol) and $Gd(O_2CMe)_3{\cdot}6H_2O$ (0.03 g, 0.2 mmol) were simultaneously added to a solution of **nanc**H_2 (0.037 g, 0.1 mmol) in MeOH/THF (8 mL, 3:1 mixture). The reaction mixture was left under magnetic stirring for approximately 1 h, until a dark brown solution was obtained. The solution was allowed to stand for ca. 16 h, filtered, and the resulting solution was allowed to undergo slow evaporation at room temperature, affording dark green crystals of **1** after 5 days. Yield 160 mg, 67% (based on the **nanc**H_2 ligand). Selected IR data (cm^{-1}): 1614, 1594, 1568, 1532, 1495, 1462, 1445, 1423, 1400, 1375, 1300, 1193, 1175, 1163, 1142, 1095, 1078, 966, 929, 896, 860, 835, 816, 793, 760, 746, 696, 647, 622, 593, 582, 561, 541, 525, 502, 480, 455, 435, 418. Elemental Analysis calc. for [$Cu^{II}(C_{22}H_{13}NO_3)$]$_n$ (**1**): C, 65.59; H, 3.25; N, 3.48. Found: C, 66.02; H, 3.48; N, 3.50%.

Single crystal X-ray diffraction: Suitable single crystals of **1** were mounted on a nylon microloop in perfluoroether oil (Paratone® N). Crystallographic data were collected on a Bruker APEX-II CCD diffractometer equipped with an Oxford Cryosystems low-temperature device operating at 150.0(1) K. Generic φ and ω scans (Mo$K\alpha$, λ = 0.71073 Å) were used for the data measurement. The diffraction patterns were indexed, and the unit cells refined with SAINT software in the Bruker APEX-II program [66]. Data reduction, scaling, and a multi-scan absorption correction were performed with SAINT and SADABS software [67,68]. Space group determination was based upon analysis of systematic absences, E statistics, and successful refinement of all structures. The structure was solved using the intrinsic phasing algorithm ShelXT [69] and refined with the least squares method by minimization of $\Sigma w(F_o^2 - F_c^2)^2$. Structure refinement and CIF compilation were carried out using SHELXL-2018 in the SHELXTL package [70]. All non-hydrogen atoms were refined anisotropically. The positions of the hydrogen atoms were calculated geometrically and refined using the riding model. The crystallographic data for **1** was deposited in the Cambridge Structural Database and assigned the following number CCDC 2222531. Crystallographic data for **1** are summarized in Table 1.

Table 1. Selected crystallographic data for **1**.

Chemical Formula	**$C_{22}H_{13}CuNO_3$**
M_r	402.87
Crystal system, space group	Orthorhombic, $P2_12_12_1$
Temperature (K)	152(1)
a, b, c (Å)	7.3981 (5), 12.0652 (10), 18.5949 (13)
V (Å^3)	1659.8 (2)
Z	4
Radiation type	Mo $K\alpha$
μ (mm^{-1})	1.34
Crystal size (mm)	0.5 × 0.5 × 0.5
T_{min}, T_{max}	0.561, 0.746
No. of measured, independent, and observed [$I > 2\sigma(I)$] reflections	12654, 4985, 4680
R_{int}	0.038
$(\sin\theta/\lambda)_{max}$ (Å^{-1})	0.715
R [$F^2 > 2\sigma(F^2)$], $wR(F^2)$, S	0.034, 0.076, 1.03
No. of reflections	4985
No. of parameters	245
H-atom treatment	H-atom parameters constrained
$\Delta\rho_{max}$, $\Delta\rho_{min}$ (e Å^{-3})	0.49, −0.35
Absolute structure	Refined as an inversion twin.
Absolute structure parameter	0.081 (15)

Magnetic susceptibility: Variable temperature magnetic data (1.8–300 K) for **1** were collected using a Quantum Design MPMS-XL SQUID magnetometer, in a magnetic field strength of 1 kOe. Field-dependent magnetic data between 0 and 50 kOe were collected at 1.8 K with several data points recollected as the field returned to zero. No evidence for hysteresis was observed. Corrections for the sample holder assembly, measured independently, diamagnetic contributions from the sample, estimated from Pascal's constants [71], and the temperature-independent paramagnetism (TIP) of Cu(II) were applied.

Computational Details: All calculations were carried out within the Jaguar 11.4 program package [72], using the B3LYP functional (Becke, three parameter, Lee−Yang−Parr hybrid functional) [73,74]. An a posteriori dispersion correction was applied using the D3 method of Grimme [75] and the LACV3P+** basis set employed [76], providing an effective core potential for the transition metal ion. A self-consistent field (1SCF) calculation was used based on a fragment of the polymer chain, comprising two Cu(II) ions, the bridging ligands, and the ligands in the immediate coordination sphere of each metal ion (Figure S1, Supplementary Materials). The strength of the exchange was determined to determine the energies and expectation values of the open shell spin triplet and broken symmetry singlet (BSS) configurations using the method of Yamaguchi (Equation (3)):

$$J = \frac{-(E_T - E_{BSS})}{< S^2 >_T - < S^2 >_{BSS}} \quad (3)$$

The initial guess explicitly stated formal charges on the Cu(II) ions and O atoms of the **nanc**$^{2-}$ ligands and the value of the spin state (2S) on each Cu(II) centre (either +1 for both Cu(II) centres for the triplet state or +1/−1 for the Cu(II) centres for the BSS configuration).

3. Results

Synthesis of nancH$_2$: The Schiff base ligand, **nanc**H$_2$ (Figure 1), was obtained in 70% yield from the reaction of 2–hydroxy–1–naphthaldehyde and 3–amino–2–naphthoic acid, Scheme 1. The ligand was subsequently characterized by ^{1}H and ^{13}C NMR, IR, and mass spectrometry (Figures S2, S3, S7 and S8).

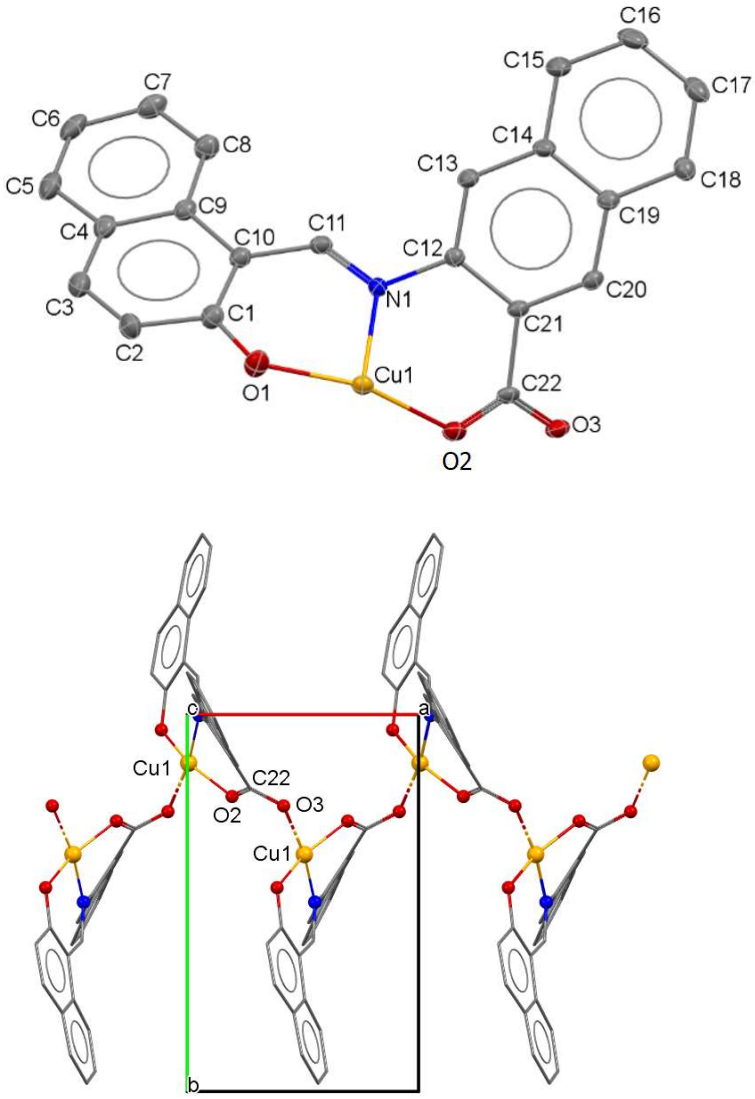

Figure 1. (**top**) ORTEP plot of the asymmetric unit of $[Cu^{II}(\mathbf{nanc})]_n$ (**1**) with the appropriate atomic labelling scheme. Thermal ellipsoids are plotted at 50% and H atoms are omitted for clarity; (**bottom**) crystal packing of **1**, view down the crystallographic *c*-axis showing the 1-D chain topology; H atoms are omitted for clarity.

Synthesis of complex 1: Cu(II)/Ln(III) coordination chemistry has been shown to provide *3d/4f* metal complexes that possess high nuclearity, interesting magnetic properties, and unique structural topologies [77–79]. Accordingly, following the serendipitous self-assembly approach, various ligand/metal ratios were explored with **nanc**H_2 and $CuCl_2/GdCl_3$, $Cu(NO_3)_2/Gd(NO_3)_3$, $Cu(ClO_4)_2/Gd(CF_3SO_3)_3$, and $Cu(O_2CMe)_2/Gd(O_2CMe)_3$ in both the presence and absence of Et_3N as the base. The reactions involving the $CuCl_2/GdCl_3$ and $Cu(NO_3)_2/Gd(NO_3)_3$ mixtures with **nanc**H_2 led to a colour change, but no crystalline product(s) were isolated from the filtrate. The reactions of **nanc**H_2 with $Cu(ClO_4)_2/Gd(CF_3SO_3)_3$ provided brown oils and/or yellow powder (attributed to unreacted **nanc**H_2 ligand based on tlc and the ^{1}H NMR data). Numerous different $Cu(O_2CMe)_2/Gd(O_2Cme)_3/$**nanc**$H_2/Et_3N$ ratios were investigated, but again deposited **nanc**H_2 as a yellow powder, indicating that the **nanc**H_2 ligand was not coordinating to the metal ions. Conversely, in the absence of Et_3N, the room temperature reaction of $Cu(O_2Cme)_2$, $Gd(O_2Cme)_3$, and **nanc**H_2, in a 1:2:1 ratio, afforded dark green crystals of **1** after several days which were found to be air stable. Although **1** does not contain Gd(III) ions, the presence of $Gd(O_2CMe)_3$ during

the synthesis appeared crucial since attempts to isolate the Cu(II) coordination polymer **1** without the addition of a Gd(III) salt afforded no isolable products, both in the presence and absence of Et_3N. Similarly, the use of $Gd(O_2Cme)_3$ in a 1:1 ratio with $Cu(O_2Cme)_2$ also proved unsuccessful, confirming the need for a 1:2 ratio between these two metal salts. The Gd(III) ions may serve to deprotonate the **nanc**H_2 ligand (especially in the absence of Et_3N) and/or abstract acetate from $Cu(O_2Cme)_2$, with formation of a $[Gd(O_2Cme)_4]^-$ 'ate complex, activating the Cu(II) centre with respect to attack by **nanc**H_2.

Crystal structure of 1: Dark green crystals of **1** were obtained from reaction of $Cu(O_2Cme)_2$, $Gd(O_2Cme)_3$, and **nanc**H_2 by slow evaporation of the mother liquor. Compound **1** crystalizes in the orthorhombic space group $P2_12_12_1$ with one Cu(**nanc**) unit in the asymmetric unit. The structure of the asymmetric unit, along with a portion of the polymer chain of **1,** are presented in Figure 1. Selected bond distances and angles are listed in Table 2. In the asymmetric unit, a Cu(II) ion is coordinated by a doubly deprotonated **nanc**$^{2-}$ ligand. A symmetry-related O3 atom completes the fourth coordination site, leading to a distorted square planar Cu(II) centre, where the sum of the angles (ranging from 87.21(9)–93.17(9)°, Table 2) is 363.76°. The distorted square planar geometry is further confirmed by the τ_4 descriptor for 4-coordination, which is 0.22 for **1**, i.e., much closer to 0.00 for idealized square planar geometry than to 1.00 for tetrahedral [80]. The tetrahedrality calculated for complex **1** gives a dihedral angle of 22.67° (for strictly square planar complexes with D_{4h} symmetry the tetrahedrality is 0°; for tetrahedral complexes with D_{2d} symmetry the tetrahedrality equals 90°), again supporting a distorted square planar geometry for the basal CuO_3N plane [81]. The **nanc**$^{2-}$ ligand and the Cu(II) centre are far from co-planar, as evidenced by the dihedral angles of 38.65° and 31.18° between the two naphthalene moieties of the **nanc**$^{2-}$ ligand and the coordination plane of the Cu(II) ion. The molecule crystallizes in a chiral space group, with the polymer chains propagating parallel to the crystallographic *a*-axis. Neighbouring Cu1 ions are bridged via a carboxylato group that adopts a syn, anti-η^1:η^1:μ bidentate bridging mode, resulting in the formation of a 1D chain (Figure 1, bottom). This coordination mode provides a non-planar Cu1-O2-C22-O3-Cu1 bridge, and a Cu1$\cdots$Cu1 intrachain distance of 4.902(5) Å. Detailed analysis of the crystal packing reveals there are no classical H-bonds, but there are C-H$\cdots\pi$ interactions involving an aromatic C-H donor of one molecule and an aromatic π-acceptor of a neighbouring molecule. For example, C-H$\cdots\pi$ distances for C-H(18)$\cdots$Ar(C1C2C3C4C9C10) and C-H(15)$\cdots$Ar(C12,C13,C14,C19,C20) were found to be 2.539 Å and 2.199 Å, respectively.

Table 2. Selected geometric parameters (Å, °) for **1**.

Cu1—O1	1.890 (2)	Cu1—O3^{i}	1.947 (2)
Cu1—N1	1.933 (2)	O3—Cu1^{ii}	1.9469 (19)
Cu1—O2	1.943 (2)		
O1—Cu1—N1	92.29 (9)	O1—Cu1—O3^{i}	87.21 (9)
O1—Cu1—O2	159.44 (10)	N1—Cu1—O3^{i}	169.02 (9)
N1—Cu1—O2	93.17 (9)	O2—Cu1—O3^{i}	91.09 (9)

Symmetry code(s): (i) $x-\frac{1}{2}, -y+\frac{1}{2}, -z+1$; (ii) $x+\frac{1}{2}, -y+\frac{1}{2}, -z+1$.

Magnetic properties of 1: M(H) measurements for **1** at 1.8 K revealed no hysteresis (Figure S6), consistent with previous observations that linear S = $\frac{1}{2}$ chains do not show long-range order [82]. The saturation moment of 6300 emu/mol is consistent with an $S = \frac{1}{2}$ ion with g-value of 2.2.

The variable temperature dc susceptibility data for **1** reveal the compound displays Curie–Weiss behaviour (45–300 K) with C = 0.474(1) Oe^{-1} emu K mol^{-1} and θ = +7.9(3) K (Figure 2, inset). The Curie constant is consistent with $S = \frac{1}{2}$ and g = 2.248, while the positive Weiss constant is consistent with the presence of local ferromagnetic exchange. The value of $\chi_m T$ (Figure 2) at room temperature (0.484 emu K mol^{-1} Oe^{-1}) is consistent with the Curie constant and increases upon cooling down to 1.8 K, in agreement with the

positive nature of the Weiss constant. A first estimate of the exchange coupling can be derived from the mean field model which relates the microscopic exchange coupling (J) to the macroscopic Weiss constant (θ) according to Equation (4), where z = number of nearest neighbours, which is 2 for a linear chain. Based on Equation (4), a first estimate of J/k is +15.8 K (11 cm^{-1}):

$$\theta = zJS(S + 1)/3k \quad (4)$$

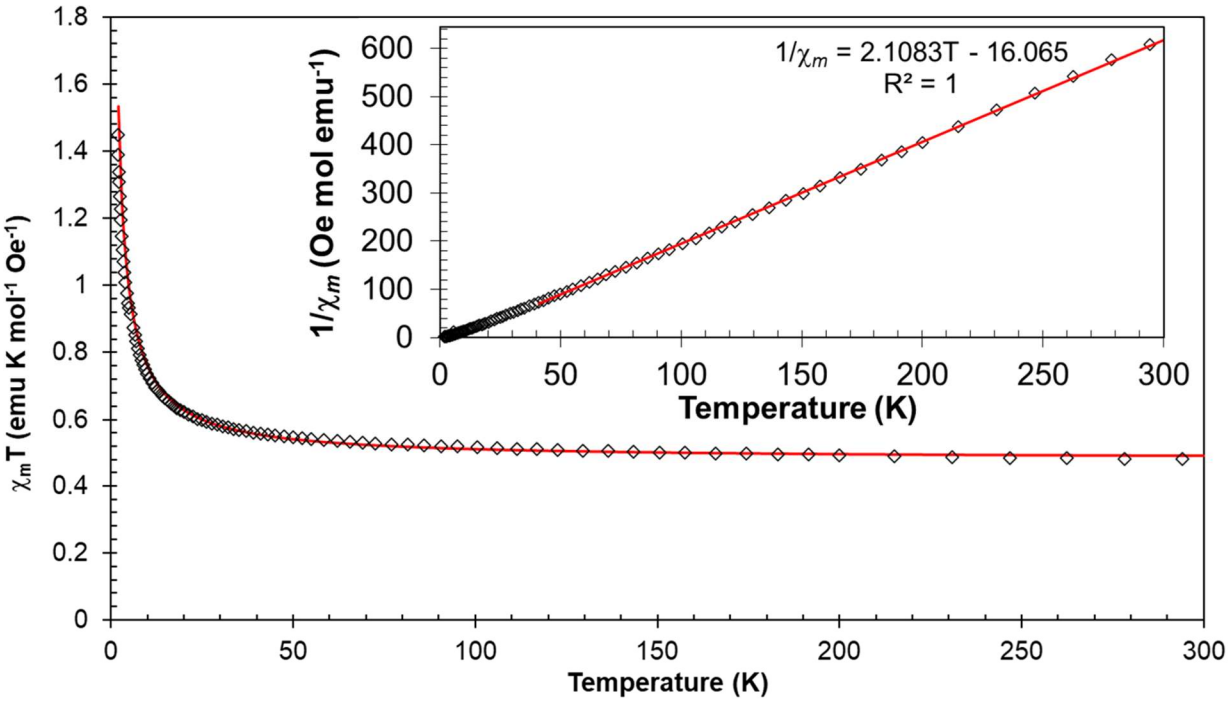

Figure 2. Temperature dependence of $\chi_m T$ for **1.** The red solid line represents the best fit to the uniform Heisenberg 1D-ferromagnetic chain model. The inset displays the temperature dependence of $1/\chi_m$ for **1.** The red solid line represents the fit to the Curie–Weiss law (40–300 K).

A more analytical approach to model the exchange within the polymer is to implement Equation (1) for the 1D quantum Heisenberg ferromagnetic chain model (1D QHFM), Equation (1) [30] which implements the $H = -JS_i.S_j$ Hamiltonian (Equation (2)). The fit to the 1D QHFM model is presented in Figure 2 (and Figure S5, Supporting Information). The best-fit provides an exchange parameter of J/k = +12.3 K and g = 2.271. The sign and magnitude of the exchange was also estimated using DFT on a model 'dimer' structure (Figure S1), extracted from the polymer chain which replicated the coordination environment of the two Cu(II) ions and the geometry of the bridging ligand.

DFT studies of 1: The strength of the exchange was also computationally determined at the B3LYP-D3/LACV3P*++ level of theory using Yamaguchi's expression for the exchange (Equation (3)) [83,84], based on the computed energies and expectation values for the triplet and broken symmetry singlet configurations [85,86]. This afforded J/k = +13.8 K good agreement with that determined from fitting the magnetic data to the 1D QHFM model.

The syn, anti bridging mode has been identified to promote either weak ferromagnetic or antiferromagnetic exchange in carboxylato-bridged Cu(II) complexes [87]. However, as the Cu-O-C-O-Cu exchange pathway further deviates from planarity, the ferromagnetic contribution to the exchange parameter J is seen to increase, while the antiferromagnetic contribution is reduced, owing to the reduction in the overlap between the magnetic orbitals of the copper atoms via the syn, anti carboxylato group [88–92]. Thus, the non-planar Cu-O-C-O-Cu exchange pathway of **1** is consistent with the ferromagnetic behaviour revealed by the magnetic measurements.

4. Conclusions

A 1D Cu(II) polymer containing the new tetradentate Schiff base ligand, N-(2′-hydroxy-1′-naphthylidene)-3-amino-2-naphthoic acid (**nanc**H_2) has been synthesized and magneto-structurally characterized. The molecular structure comprises distorted square planar Cu(II) ions linked via syn, anti- carboxylate bridges of the nanc^{2-} chelate. Analysis of the dc magnetic data reveals the presence of moderate ferromagnetic exchange interactions between the $S = \frac{1}{2}$ metal centers. In this respect, the magnetic data fit well to a 1D quantum Heisenberg ferromagnetic (QHFM) chain with a g = 2.271 and J = +12.3 K. The experimental data are further supported by DFT calculations, where implementing the broken symmetry approach on a model dimeric unit extracted from the 1D chain, afforded an exchange coupling J = +13.8 K. These first preliminary results from the study of the coordination affinity of nanc^{2-} towards both 3*d*- and 4*f*-metal ions highlights the binding preference of nanc^{2-} for Cu(II) over Gd(III) ions. Work in progress is focused on the realization of this trend by employing different, redox-active, or inert 3*d*-metal ions and trivalent lanthanide ions.

Supplementary Materials: The following supporting information can be downloaded at: https://www.mdpi.com/article/10.3390/chemistry5010007/s1, Figure S1: Structural model used for **1** when performing DFT calculations to elucidate the theoretical value of the magnetic exchange parameter J.; Figure S2. Infrared spectra obtained for the N-naphthalidene-2-amino-naphthoic acid (nancH2) ligand; Figure S3. Mass spectra obtained for the N-naphthalidene-2-amino-naphthoic acid (nancH2) ligand, in a DCM/MeOH solvent mixture; Figure S4. Infrared spectra obtained for **1**; Figure S5. Temperature dependence of 1/χm for **1**; Figure S6. Field/Temperature dependence of M for **1**; Figure S7. 1H NMR spectrum of the N-naphthalidene-2-amino-naphthoic acid (nancH2) ligand in DMSO-d6; Figure S8. 13C NMR spectrum of the N-naphthalidene-2-amino-naphthoic acid (nancH2) ligand in DMSO-d6.

Author Contributions: Conceptualization, M.P. and T.C.S.; investigation A.W., G.D.M., M.M.T., J.M.R. and M.P.; resources M.P. and M.M.T.; writing-original draft preparation, A.W., J.M.R. and M.P.; writing-review and editing, A.W., G.D.M., J.M.R., M.M.T. and M.P.; supervision, M.P. and J.M.R.; funding acquisition, J.M.R., M.M.T. and M.P. All authors have read and agreed to the published version of the manuscript.

Funding: M.P. and J.M.R. would like to thank NSERC for financial support through the NSERC Discovery (DG) and Research Tools and Instruments (RTI) programs; 2018-04255 (RTI M.P.); 2017-00091 (DG M.P.); 2020-04627 (DG J.M.R.). A.W. would like to acknowledge the support of NSERC through the Postgraduate Scholarships—Doctoral (PGS D) program. M.M.T. gratefully acknowledges financial assistance from the NSF (IMR-0314773) and the Kresge Foundation toward the purchase of the MPMS SQUID magnetometer.

Institutional Review Board Statement: Not applicable.

Informed Consent Statement: Not applicable.

Data Availability Statement: The crystallographic data for **1** has been deposited in the Cambridge Structural Database and assigned the following number CCDC 2222531. It can be available for download free of charge at https://www.ccdc.cam.ac.uk/structures/ (accessed on 30 October 2022).

Conflicts of Interest: There are no conflict to declare.

References

1. Kaliyappan, T.; Kannan, P. Co-Ordination Polymers. *Prog. Polym. Sci.* **2000**, *25*, 343–370. [CrossRef]
2. Ma, B.-Q.; Gao, S.; Su, G.; Xu, G.-X. Cyano-Bridged 4f–3d Coordination Polymers with a Unique Two-Dimensional Topological Architecture and Unusual Magnetic Behavior. *Angew. Chem. Int. Ed.* **2001**, *40*, 434–437. [CrossRef]
3. Zheng, Y.-Z.; Tong, M.-L.; Zhang, W.-X.; Chen, X.-M. Assembling Magnetic Nanowires into Networks: A Layered Co^{II} Carboxylate Coordination Polymer Exhibiting Single-Chain-Magnet Behavior. *Angew. Chem. Int. Ed.* **2006**, *45*, 6310–6314. [CrossRef] [PubMed]
4. Liu, C.-M.; Zhang, D.-Q.; Zhu, D.-B. 1D Coordination Polymers Constructed from Anti–anti Carboxylato-Bridged $Mn^{III}_3O(Brppz)_3$ Units: From Long-Range Magnetic Ordering to Single-Chain Magnet Behaviors. *Inorg. Chem.* **2009**, *48*, 4980–4987. [CrossRef] [PubMed]

5. Herringer, S.N.; Deumal, M.; Ribas-Arino, J.; Novoa, J.J.; Landee, C.P.; Wikaira, J.L.; Turnbull, M.M. S=1/2 One-Dimensional Random-Exchange Ferromagnetic Zigzag Ladder, Which Exhibits Competing Interactions in a Critical Regime. *Eur. J. Chem.* **2014**, *20*, 8355–8362. [CrossRef] [PubMed]
6. Liu, X.; Sun, L.; Zhou, H.; Cen, P.; Jin, X.; Xie, G.; Chen, S.; Hu, Q. Single-Ion-Magnet Behavior in a Two-Dimensional Coordination Polymer Constructed from Co^{II} Nodes and a Pyridylhydrazone Derivative. *Inorg. Chem.* **2015**, *54*, 8884–8886. [CrossRef]
7. Jochim, A.; Lohmiller, T.; Rams, M.; Böhme, M.; Ceglarska, M.; Schnegg, A.; Plass, W.; Näther, C. Influence of the Coligand onto the Magnetic Anisotropy and the Magnetic Behavior of One-Dimensional Coordination Polymers. *Inorg. Chem.* **2020**, *59*, 8971–8982. [CrossRef]
8. Hu, J.-J.; Peng, Y.; Liu, S.-J.; Wen, H.-R. Recent Advances in Lanthanide Coordination Polymers and Clusters with Magnetocaloric Effect or Single-Molecule Magnet Behavior. *Dalton Trans.* **2021**, *50*, 15473–15487. [CrossRef]
9. Rogge, S.M.J.; Bavykina, A.; Hajek, J.; Garcia, H.; Olivos-Suarez, A.I.; Sepúlveda-Escribano, A.; Vimont, A.; Clet, G.; Bazin, P.; Kapteijn, F.; et al. Metal–Organic and Covalent Organic Frameworks as Single-Site Catalysts. *Chem. Soc. Rev.* **2017**, *46*, 3134–3184. [CrossRef]
10. Wu, M.-X.; Yang, Y.-W. Metal-Organic Framework (MOF)-Based Drug/Cargo Delivery and Cancer Therapy. *Adv. Mater.* **2017**, *29*, 1606134. [CrossRef]
11. Dzhardimalieva, G.; Uflyand, I.E. Design and Synthesis of Coordination Polymers with Chelated Units and Their Application in Nanomaterials Science. *RSC Adv.* **2017**, *7*, 42242–42288. [CrossRef]
12. Acar, Y.; Coban, M.B.; Gungor, E.; Kara, H. Two New NIR Luminescencent Er(III) Coordination Polymers with Potential Application Optical Amplification Devices. *J. Clust. Sci.* **2020**, *31*, 117–124. [CrossRef]
13. Liu, J.-Q.; Luo, Z.-D.; Pan, Y.; Kumar Singh, A.; Trivedi, M.; Kumar, A. Recent Developments in Luminescent Coordination Polymers: Designing Strategies, Sensing Application and Theoretical Evidences. *Coord. Chem. Rev.* **2020**, *406*, 213145. [CrossRef]
14. Li, Y.-M.; Xiao, C.-Y.; Zhang, X.-D.; Xu, Y.-Q.; Lun, H.-J.; Niu, J.-Y. Mn^{II}, Cu^{II} and Co^{II} Coordination Polymers Showing Antiferromagnetism, and the Coexistence of Spin Frustration and Long Range Magnetic Ordering. *CrystEngComm* **2013**, *15*, 7756. [CrossRef]
15. Nath, A.; Islam, S.S.; Mukharjee, P.K.; Nath, R.; Mandal, S. Reentrant Spin-Glass Behavior in Cobalt(II) Based Coordination Polymers. *Cryst. Growth Des.* **2019**, *19*, 6463–6471. [CrossRef]
16. Journaux, Y.; Ferrando-Soria, J.; Pardo, E.; Ruiz-Garcia, R.; Julve, M.; Lloret, F.; Cano, J.; Li, Y.; Lisnard, L.; Yu, P.; et al. Design of Magnetic Coordination Polymers Built from Polyoxalamide Ligands: A Thirty Year Story. *Eur. J. Inorg. Chem.* **2018**, *2018*, 228–247. [CrossRef]
17. Veríssimo, L.M.; Pereira, M.S.S.; Strečka, J.; Lyra, M.L. Kosterlitz-Thouless and Gaussian Criticalities in a Mixed Spin-(1/2, 5/2, 1/2) Heisenberg Branched Chain with Exchange Anisotropy. *Phys. Rev. B* **2019**, *99*, 134408. [CrossRef]
18. Keene, T.D.; Hursthouse, M.B.; Price, D.J. Two-Dimensional Metal−Organic Frameworks: A System with Competing Chelating Ligands. *Cryst. Growth Des.* **2009**, *9*, 2604–2609. [CrossRef]
19. Saines, P.J.; Bristowe, N.C. Probing Magnetic Interactions in Metal–Organic Frameworks and Coordination Polymers Microscopically. *Dalton Trans.* **2018**, *47*, 13257–13280. [CrossRef] [PubMed]
20. Chiari, B.; Hatfield, W.E.; Piovesana, O.; Tarantelli, T.; Ter Haar, L.W.; Zanazzi, P.F. Exchange Interaction in Multinuclear Transition-Metal Complexes. 3. Synthesis, x-Ray Structure, and Magnetic Properties of $Cu_2L(CH_3COO)_2.2CH_3OH$ (L^{2-} = Anion of N,N′-Bis((2-(o-Hydroxybenzhydrylidene)Amino)Ethyl)-1,2-Ethanediamine), a One-Dimensional Heisenberg Antiferromagnet Having through-Bond Coupled Copper(II) Ions. *Inorg. Chem.* **1983**, *22*, 1468–1473. [CrossRef]
21. Gao, E.-Q.; Bai, S.-Q.; Yue, Y.-F.; Wang, Z.-M.; Yan, C.-H. New One-Dimensional Azido-Bridged Manganese(II) Coordination Polymers Exhibiting Alternating Ferromagnetic−Antiferromagnetic Interactions: Structural and Magnetic Studies. *Inorg. Chem.* **2003**, *42*, 3642–3649. [CrossRef]
22. Papatriantafyllopoulou, C.; Zartilas, S.; Manos, M.J.; Pichon, C.; Clérac, R.; Tasiopoulos, A.J. A Single-Chain Magnet Based on Linear $[Mn^{III}_2Mn^{II}]$ Units. *Chem. Commun.* **2014**, *50*, 14873–14876. [CrossRef]
23. Zhang, Y.-Z.; Dolinar, B.S.; Liu, S.; Brown, A.J.; Zhang, X.; Wang, Z.-X.; Dunbar, K.R. Enforcing Ising-like Magnetic Anisotropy via Trigonal Distortion in the Design of a W(V)–Co(II) Cyanide Single-Chain Magnet. *Chem. Sci.* **2018**, *9*, 119–124. [CrossRef]
24. Monroe, J.C.; Landee, C.P.; Turnbull, M.M.; Wikaira, J.L. Well-Isolated Pyrazine-Bridged Copper(II) Chains: Synthesis and Magneto-Structural Analysis. *J. Coord. Chem.* **2020**, *73*, 2645–2663. [CrossRef]
25. Amaral, S.; Jensen, W.E.; Landee, C.P.; Turnbull, M.M.; Matthew Woodward, F. Quantum Linear Magnetic Chains: Structure and Magnetic Behavior of (2-Methylpyrazine)Copper(II) Nitrate. *Polyhedron* **2001**, *20*, 1317–1322. [CrossRef]
26. Breunig, O.; Garst, M.; Klümper, A.; Rohrkamp, J.; Turnbull, M.M.; Lorenz, T. Quantum Criticality in the spin-1/2 Heisenberg chain system copper pyrazine dinitrate. *Sci. Adv.* **2017**, *3*, eaao3773. [CrossRef] [PubMed]
27. Bethe, H. Zur Theorie der Metalle: I. Eigenwerte und Eigenfunktionen der linearen Atomkette. *Z. Physik* **1931**, *71*, 205–226. [CrossRef]
28. Eggert, S.; Affleck, I.; Takahashi, M. Susceptibility of the Spin 1/2 Heisenberg Antiferromagnetic Chain. *Phys. Rev. Lett.* **1994**, *73*, 332–335. [CrossRef] [PubMed]
29. Johnston, D.C.; Kremer, R.K.; Troyer, M.; Wang, X.; Klümper, A.; Bud'ko, S.L.; Panchula, A.F.; Canfield, P.C. Thermodynamics of Spin S=1/2 Antiferromagnetic Uniform and Alternating-Exchange Heisenberg Chains. *Phys. Rev. B* **2000**, *61*, 9558–9606. [CrossRef]

30. Landee, C.P.; Turnbull, M.M. Review: A Gentle Introduction to Magnetism: Units, Fields, Theory, and Experiment. *J. Coord. Chem.* **2014**, *67*, 375–439. [CrossRef]
31. Landee, C.P.; Turnbull, M.M. Recent Developments in Low-Dimensional Copper(II) Molecular Magnets. *Eur. J. Inorg. Chem.* **2013**, *2013*, 2266–2285. [CrossRef]
32. Zhang, X.X.; Chui, S.S.-Y.; Williams, I.D. Cooperative Magnetic Behavior in the Coordination Polymers $[Cu_3(TMA)_2L_3]$ (L=H_2O, Pyridine). *J. Appl. Phys.* **2000**, *87*, 6007–6009. [CrossRef]
33. Kirkman-Davis, E.; Witkos, F.E.; Selmani, V.; Monroe, J.C.; Landee, C.P.; Turnbull, M.M.; Dawe, L.N.; Polson, M.I.J.; Wikaira, J.L. Pyrazine-Bridged Cu(II) Chains: Diaquabis(n-Methyl-2-Pyridone)Copper(II) Perchlorate Complexes. *Dalton Trans.* **2020**, *49*, 13693–13703. [CrossRef]
34. Santoro, A.; Mighell, A.D.; Reimann, C.W. The Crystal Structure of a 1:1 Cupric Nitrate–Pyrazine Complex $Cu(NO_3)_2 \cdot (C_4N_2H_4)$. *Acta Cryst. B* **1970**, *26*, 979–984. [CrossRef]
35. Kono, Y.; Sakakibara, T.; Aoyama, C.P.; Hotta, C.; Turnbull, M.M.; Landee, C.P.; Takano, Y. Field-Induced Quantum Criticality and Universal Temperature Dependence of the Magnetization of a Spin-1/2 Heisenberg Chain. *Phys. Rev. Lett.* **2015**, *114*, 037202. [CrossRef] [PubMed]
36. Jones, B.R.; Varughese, P.A.; Olejniczak, I.; Pigos, J.M.; Musfeldt, J.L.; Landee, C.P.; Turnbull, M.M.; Carr, G.L. Vibrational Properties of the One-Dimensional, $S = {}^1/_2$, Heisenberg Antiferromagnet Copper Pyrazine Dinitrate. *Chem. Mater.* **2001**, *13*, 2127–2134. [CrossRef]
37. Jornet-Somoza, J.; Deumal, M.; Robb, M.A.; Landee, C.P.; Turnbull, M.M.; Feyerherm, R.; Novoa, J.J. First-Principles Bottom-up Study of 1D to 3D Magnetic Transformation in the Copper Pyrazine Dinitrate S=1/2 Antiferromagnetic Crystal. *Inorg. Chem.* **2010**, *49*, 1750–1760. [CrossRef]
38. Lu, J.Y.; Babb, A.M. A Simultaneous Reduction, Substitution, and Self-Assembly Reaction under Hydrothermal Conditions Afforded the First Diiodopyridine Copper(I) Coordination Polymer. *Inorg. Chem.* **2002**, *41*, 1339–1341. [CrossRef]
39. Erxleben, A. Structures and Properties of Zn(II) Coordination Polymers. *Coord. Chem. Rev.* **2003**, *246*, 203–228. [CrossRef]
40. Horikoshi, R.; Mikuriya, M. One-Dimensional Coordination Polymers from the Self-Assembly of Copper(II) Carboxylates and 4,4′-Dithiobis(Pyridine). *Bull. Chem. Soc. Jpn.* **2005**, *78*, 827–834. [CrossRef]
41. Liu, H.-Y.; Wu, H.; Ma, J.-F.; Liu, Y.-Y.; Liu, B.; Yang, J. Syntheses, Structures, and Photoluminescence of Zinc(II) Coordination Polymers Based on Carboxylates and Flexible Bis-[(Pyridyl)-Benzimidazole] Ligands. *Cryst. Growth Des.* **2010**, *10*, 4795–4805. [CrossRef]
42. Wang, J.-P.; Su, B.; Li, J.-H.; Wang, G.-M. Diverse Architectures and Luminescence Properties of Three Low-Dimensional Zn(II)/Cd(II) Coordination Polymers Based on a Pyridine-Imidazole Ligand. *Inorg. Chem. Commun.* **2018**, *90*, 29–33. [CrossRef]
43. Kumar, S.; Dhar, D.N.; Saxena, P.N. Applications of Metal Complexes of Schiff Bases—A Review. *J. Sci. Ind. Res.* **2009**, *68*, 181–187.
44. Qin, W.; Long, S.; Panunzio, M.; Biondi, S. Schiff Bases: A Short Survey on an Evergreen Chemistry Tool. *Molecules* **2013**, *18*, 12264–12289. [CrossRef]
45. Dhahagani, K.; Mathan Kumar, S.; Chakkaravarthi, G.; Anitha, K.; Rajesh, J.; Ramu, A.; Rajagopal, G. Synthesis and Spectral Characterization of Schiff Base Complexes of Cu(II), Co(II), Zn(II) and VO(IV) Containing 4-(4-Aminophenyl)Morpholine Derivatives: Antimicrobial Evaluation and Anticancer Studies. *Spectrochim. Acta A Mol. Biomol. Spectrosc.* **2014**, *117*, 87–94. [CrossRef] [PubMed]
46. Liu, Q.; Yang, X.; Huang, Y.; Xu, S.; Su, X.; Pan, X.; Xu, J.; Wang, A.; Liang, C.; Wang, X.; et al. A Schiff Base Modified Gold Catalyst for Green and Efficient H_2 Production from Formic Acid. *Energy Environ. Sci.* **2015**, *8*, 3204–3207. [CrossRef]
47. Nair, M.S.; Arish, D.; Joseyphus, R.S. Synthesis, Characterization, Antifungal, Antibacterial and DNA Cleavage Studies of Some Heterocyclic Schiff Base Metal Complexes. *J. Saudi Chem. Soc.* **2012**, *16*, 83–88. [CrossRef]
48. Hossain, M.S.; Roy, P.K.; Zakaria, C.M.; Kudrat-E-Zahan, M. Selected Schiff Base Coordination Complexes and their Microbial Application: A Review. *Int. J. Chem. Stud.* **2018**, *6*, 19–31.
49. Kolcu, F.; Erdener, D.; Kaya, İ. A Schiff Base Based on Triphenylamine and Thiophene Moieties as a Fluorescent Sensor for Cr(III) Ions: Synthesis, Characterization and Fluorescent Applications. *Inorg. Chim. Acta.* **2020**, *509*, 119676. [CrossRef]
50. More, M.S.; Joshi, P.G.; Mishra, Y.K.; Khanna, P.K. Metal Complexes Driven from Schiff Bases and Semicarbazones for Biomedical and Allied Applications: A Review. *Mater. Today Chem.* **2019**, *14*, 100195. [CrossRef]
51. Khalaji, A.D.; Hadadzadeh, H.; Fejfarova, K.; Dusek, M. Metal-Dependent Assembly of a Tetranuclear Copper(II) Complex versus a 1D Chain Coordination Polymer of Cobalt(III) Complex with N_2O_2-Chelating Schiff-Base Ligand: Synthesis, Characterization and Crystal Structures. *Polyhedron* **2010**, *29*, 807–812. [CrossRef]
52. Ejidike, I.P.; Ajibade, P.A. Synthesis, Characterization and Biological Studies of Metal(II) Complexes of (3E)-3-[(2-{(E)-[1-(2,4-Dihydroxyphenyl)Ethylidene]Amino}ethyl)Imino]-1-Phenylbutan-1-One Schiff Base. *Molecules* **2015**, *20*, 9788–9802. [CrossRef] [PubMed]
53. Novoa, N.; Manzur, C.; Roisnel, T.; Kahlal, S.; Saillard, J.-Y.; Carrillo, D.; Hamon, J.-R. Nickel(II)-Based Building Blocks with Schiff Base Derivatives: Experimental Insights and DFT Calculations. *Molecules* **2021**, *26*, 5316. [CrossRef]
54. Protasenko, N.A.; Baryshnikova, S.V.; Astaf'eva, T.V.; Cherkasov, A.V.; Poddel'sky, A.I. Mono- and Binuclear Zinc Complexes with a Bidentate Phenol-Containing 2-Benzylideneamino-5-Methylphenol Schiff Base. *Russ. J. Coord. Chem.* **2021**, *47*, 417–423. [CrossRef]

55. Celedon, S.; Roisnel, T.; Carrillo, D.; Ledoux-Rak, I.; Hamon, J.-R.; Manzur, C. Transition Metal(II) Complexes Featuring Push-Pull Dianionic Schiff Base Ligands: Synthesis, Crystal Structure, Electrochemical, and NLO Studies. *J. Coord. Chem.* **2020**, *73*, 3079–3094. [CrossRef]
56. Ghosh, P.; Dey, S.K.; Ara, M.H.; Karim, K.; Islam, A.B.M.N. A Review on Synthesis and Versatile Applications of Some Selected Schiff Bases with Their Transition Metal Complexes. *Egypt. J. Chem.* **2019**, *62*, 523–547. [CrossRef]
57. Zare, N.; Zabardasti, A. A New Nano-Sized Mononuclear Cu(II) Complex with N,N-Donor Schiff Base Ligands: Sonochemical Synthesis, Characterization, Molecular Modeling and Biological Activity. *Appl. Organomet. Chem.* **2019**, *33*, e4687. [CrossRef]
58. El-Bindary, A.A.; El-Sonbati, A.Z.; Diab, M.A.; Ghoneim, M.M.; Serag, L.S. Polymeric Complexes—LXII. Coordination Chemistry of Supramolecular Schiff Base Polymer Complexes—A Review. *J. Mol. Liq.* **2016**, *216*, 318–329. [CrossRef]
59. Sadhukhan, D.; Ray, A.; Butcher, R.J.; Gómez García, C.J.; Dede, B.; Mitra, S. Magnetic and Catalytic Properties of a New Copper(II)–Schiff Base 2D Coordination Polymer Formed by Connected Helical Chains. *Inorg. Chim. Acta* **2011**, *376*, 245–254. [CrossRef]
60. Shi, S.-M.; Gu, Y.-Q.; Chen, Z.-F.; Liu, Y.-C.; Liang, H. One-Dimensional Chain Copper(II) and Nickel(II) Coordination Polymers With N-Salicylideneglycine Schiff Base Ligand. *Synth. React. Inorg. M* **2012**, *42*, 1262–1266. [CrossRef]
61. İnci, D.; Aydın, R.; Zorlu, Y. NOO-Type Tridentate Schiff Base Ligand and Its One-Dimensional Cu(II) Coordination Polymer: Synthesis, Crystal Structure, Biomacromolecular Interactions and Radical Scavenging Activities. *Inorg. Chim. Acta* **2021**, *514*, 119994. [CrossRef]
62. Nabei, A.; Kuroda-Sowa, T.; Okubo, T.; Maekawa, M.; Munakata, M. The Effect of Molecular Packing on the Occurrence of Spin Crossover Phenomena in One-Dimensional Fe(II)-Bis-Schiff Base Complexes. *Inorg. Chim. Acta* **2008**, *361*, 3489–3493. [CrossRef]
63. Choi, S.W.; Kwak, H.Y.; Yoon, J.H.; Kim, H.C.; Koh, E.K.; Hong, C.S. Intermolecular Contact-Tuned Magnetic Nature in One-Dimensional 3d−5d Bimetallic Systems: From a Metamagnet to a Single-Chain Magnet. *Inorg. Chem.* **2008**, *47*, 10214–10216. [CrossRef] [PubMed]
64. Lee, J.; Lim, K.; Yoon, J.; Ryu, D.; Koo, B.; Koh, E.; Hong, C. Cyanide-Bridged $W^{V}Mn^{III}$ Single-Chain Magnet Based on an Octacoordinate $[W(CN)_6(Phen)]^-$ Anion. *Sci. China Chem.* **2012**, *55*, 1012–1017. [CrossRef]
65. Lochenie, C.; Gebauer, A.; Klimm, O.; Puchtler, F.; Weber, B. Iron(II) Spin Crossover Complexes with Diaminonaphthalene-Based Schiff Base-like Ligands: 1D Coordination Polymers. *New J. Chem.* **2016**, *40*, 4687–4695. [CrossRef]
66. *APEX Suite of Crystallographic Software*, APEX 2 Version 4; Bruker AXS Inc.: Madison, WI, USA, 2008.
67. *Bruker SAINT*, version V8.34A; Bruker AXS Inc.: Madison, WI, USA, 2013.
68. Sheldrick, G.M. *SADABS*, version 2.03; University of Göttingen: Göttingen, Germany, 2002.
69. Sheldrick, G.M. *SHELXT*—Integrated Space-Group and Crystal-Structure Determination. *Acta Crystallogr. A Found. Adv.* **2015**, *71*, 3–8. [CrossRef]
70. Sheldrick, G.M. Crystal Structure Refinement with *SHELXL*. *Acta Crystallogr. C Struct. Chem.* **2015**, *71*, 3–8. [CrossRef]
71. Carlin, R.L. *Magnetochemistry*; Springer: Berlin/Heidelberg, 1986; ISBN 9783642707353 9783642707339.
72. *Jaguar*, version 11.4; Schrödinger, Inc.: New York, NY, USA, 2021.
73. Becke, A.D. A New Mixing of Hartree–Fock and Local Density-functional Theories. *J. Chem. Phys.* **1993**, *98*, 1372–1377. [CrossRef]
74. Lee, C.; Yang, W.; Parr, R.G. Development of the Colle-Salvetti Correlation-Energy Formula into a Functional of the Electron Density. *Phys. Rev. B* **1988**, *37*, 785–789. [CrossRef]
75. Grimme, S.; Antony, J.; Ehrlich, S.; Krieg, H. A Consistent and Accurate Ab Initio Parametrization of Density Functional Dispersion Correction (DFT-D) for the 94 Elements H-Pu. *J. Chem. Phys.* **2010**, *132*, 154104. [CrossRef]
76. Hay, P.J.; Wadt, W.R. Ab Initio Effective Core Potentials for Molecular Calculations. Potentials for K to Au Including the Outermost Core Orbitals. *J. Chem. Phys.* **1985**, *82*, 299–310. [CrossRef]
77. Wu, J.; Zhao, L.; Zhang, L.; Li, X.-L.; Guo, M.; Powell, A.K.; Tang, J. Macroscopic Hexagonal Tubes of 3d-4f Metallocycles. *Angew. Chem. Int. Ed.* **2016**, *55*, 15574–15578. [CrossRef] [PubMed]
78. Langley, S.K.; Chilton, N.F.; Moubaraki, B.; Hooper, T.; Brechin, E.K.; Evangelisti, M.; Murray, K.S. Molecular Coolers: The Case for $[Cu^{II}_5Gd^{III}_4]$. *Chem. Sci.* **2011**, *2*, 1166. [CrossRef]
79. Leng, J.-D.; Liu, J.-L.; Tong, M.-L. Unique Nanoscale $\{Cu^{II}_{36}Ln^{III}_{24}\}$ (Ln = Dy and Gd) Metallo-Rings. *Chem. Commun.* **2012**, *48*, 5286. [CrossRef]
80. Yang, L.; Powell, D.R.; Houser, R.P. Structural Variation in Copper(I) Complexes with Pyridylmethylamide Ligands: Structural Analysis with a New Four-Coordinate Geometry Index, τ_4. *Dalton Trans.* **2007**, *9*, 955–964. [CrossRef]
81. Casanova, J.; Alzuet, G.; Ferrer, S.; Latorre, J.; Antonio Ramírez, J.; Borrás, J. Superoxide Dismutase Activity of Ternary Copper Complexes of Sulfathiazole and Imidazole Derivatives. Synthesis and Properties of $[CuL_2(R\text{-}Him)_2]$ [HL=4-Amino-N-(Thiazol-2-Yl)Benzenesulfonamide, R-Him=4-Methylimidazole, 4,4-Dimethylimidazoline or 1,2-Dimethylimidazole]. Crystal Structure of $[CuL_2$(4,4-Dimethylimidazoline)2]. *Inorg. Chim. Acta* **2000**, *304*, 170–177. [CrossRef]
82. Blundell, S. *Magnetism in Condensed Matter*; Oxford master series in condensed matter physics; Oxford University Press: New York, NY, USA, 2001; pp. 171–172. ISBN 9780198505914.
83. Yamaguchi, K.; Takahara, Y.; Fueno, T. Ab-Initio Molecular Orbital Studies of Structure and Reactivity of Transition Metal-OXO Compounds. In *Applied Quantum Chemistry*; Smith, V.H., Schaefer, H.F., Morokuma, K., Eds.; Springer: Dordrecht, The Netherlands, 1986; pp. 155–184. ISBN 9789401086097 9789400947467.

84. Soda, T.; Kitagawa, Y.; Onishi, T.; Takano, Y.; Shigeta, Y.; Nagao, H.; Yoshioka, Y.; Yamaguchi, K. Ab Initio Computations of Effective Exchange Integrals for H–H, H–He–H and Mn_2O_2 Complex: Comparison of Broken-Symmetry Approaches. *Chem. Phys. Lett.* **2000**, *319*, 223–230. [CrossRef]
85. Ruiz, E.; Cano, J.; Alvarez, S.; Alemany, P. Broken Symmetry Approach to Calculation of Exchange Coupling Constants for Homobinuclear and Heterobinuclear Transition Metal Complexes. *J. Comput. Chem.* **1999**, *20*, 1391–1400. [CrossRef]
86. Onofrio, N.; Mouesca, J.-M. Analysis of the Singlet–Triplet Splitting Computed by the Density Functional Theory–Broken-Symmetry Method: Is It an Exchange Coupling Constant? *Inorg. Chem.* **2011**, *50*, 5577–5586. [CrossRef]
87. Ruiz-Pérez, C.; Sanchiz, J.; Molina, M.H.; Lloret, F.; Julve, M. Ferromagnetism in Malonato-Bridged Copper(II) Complexes. Synthesis, Crystal Structures, and Magnetic Properties of $\{[Cu(H_2O)_3][Cu(Mal)_2(H_2O)]\}_n$ and $\{[Cu(H_2O)_4]_2[Cu(Mal)_2(H_2O)]\}[Cu(Mal)_2(H_2O)_2]\{[Cu(H_2O)_4][Cu(Mal)_2(H_2O)_2]\}$ (H_2mal=Malonic Acid). *Inorg. Chem.* **2000**, *39*, 1363–1370. [CrossRef]
88. Towle, D.K.; Hoffmann, S.K.; Hatfield, W.E.; Singh, P.; Chaudhuri, P. Magnetic and Structural Properties of Acetato(Dien)Copper(1+) Perchlorate: A μ-Acetato-Bridged Quasi-One-Dimensional Complex. *Inorg. Chem.* **1988**, *27*, 394–399. [CrossRef]
89. Colacio, E.; Costes, J.P.; Kivekas, R.; Laurent, J.P.; Ruiz, J. A Quasi-Tetrahedral Tetracopper Cluster with Syn-Anti Bridging Carboxylate Groups: Crystal and Molecular Structure and Magnetic Properties. *Inorg. Chem.* **1990**, *29*, 4240–4246. [CrossRef]
90. Colacio, E.; Dominguez-Vera, J.M.; Costes, J.P.; Kivekas, R.; Laurent, J.P.; Ruiz, J.; Sundberg, M. Structural and Magnetic Studies of a Syn-Anti Carboxylate-Bridged Helix-like Chain Copper(II) Complex. *Inorg. Chem.* **1992**, *31*, 774–778. [CrossRef]
91. Colacio, E.; Dominguez-Vera, J.M.; Moreno, J.M.; Ruiz, J.; Kivekäs, R.; Romerosa, A. Structure and Magnetic Properties of a Syn-Anti Carboxylate Bridged Linear Trinuclear Copper(II) Complex with Ferromagnetic Exchange Interaction. *Inorg. Chim. Acta* **1993**, *212*, 115–121. [CrossRef]
92. Konar, S.; Mukherjee, P.S.; Drew, M.G.B.; Ribas, J.; Ray Chaudhuri, N. Syntheses of Two New 1D and 3D Networks of Cu(II) and Co(II) Using Malonate and Urotropine as Bridging Ligands: Crystal Structures and Magnetic Studies. *Inorg. Chem.* **2003**, *42*, 2545–2552. [CrossRef] [PubMed]